JOURNAL OF MATERIALS SCIENCE 29 (1994) 5680–5688

DSC and DMA studies of particulate reinforced metal matrix composites

T. DAS, S. BANDYOPADHYAY, S. BLAIRS
School of Materials Science and Engineering, University of New South Wales, Sydney 2052, Australia

Thermal studies have been carried out on a series of particulate (SiC and Al_2O_3) reinforced 6061 Al metal matrix composites. Differential scanning calorimetry and dynamic mechanical analysis have provided information on the formation/dissolution of precipitate phase(s) and the effect of temperature on the short-term storage modulus of the materials, respectively. These studies were also used to identify the phase changes responsible for the maximum damping properties of the materials.

1. Introduction

Particulate reinforced aluminium metal matrix composites (PMMC) are receiving increasing attention as potential light weight engineering materials [1, 2]. Heat-treatable alloys, such as 6061, have been used extensively as the matrix materials in such composites. In these alloys the maximum strength is developed by precipitation of a fine phase dispersed throughout the matrix, obtained by quenching after solution heat-treatment in the single-phase region (α), followed by heating to a moderate temperature for a certain length of time. Formation of such precipitates is often believed to be enhanced/accelerated by the reinforcing particles [3, 4].

In recently reported work thermal analysis techniques, like differential scanning calorimetry (DSC), have been employed to study the change in enthalpy/specific heat which is considered to be associated with formation/dissolution of the precipitates [5–9]. Such studies have added a new dimension in understanding the role of particulate reinforcement in PMMC materials.

Dynamic mechanical analysis (DMA) is another thermal analysis technique which can be used to study, in particular, changes in the (short-term) storage modulus as a function of temperature, as well as in obtaining other information, such as damping characteristics [10–14].

As part of a broad research program, the present authors have used DSC and DMA techniques to study microstructural/physical characterization of a series of PMMC materials, and the results obtained so far constitute the subject matter of this report.

2. Experimental procedure

Materials used in this study were as follows: (1) 10 vol % SiC/6061; (2) 20 vol % SiC/6061; (3) 10 vol % Al_2O_3/6061; (4) 15 vol % Al_2O_3/6061; (5) 20 vol % Al_2O_3/6061; (6) 20 vol % Al_2O_3 (Microsphere)/6061 (Comral-85); (7) 6061, unreinforced. Representative microstructures of composites 1–6 are provided in Figs 1–6 respectively. The particle size and size distribution of materials 1–3, 5 and 6 are given elsewhere [15]. All materials were provided by Comalco Research Centre of Thomastown, Victoria; composites 1–5 were obtained from commercial sources in the form of billets which were then extruded down to approximately 19 mm diameter rods; material 6 was a composite developed by Comalco. Material 6 and unreinforced 6061 were both supplied as extruded 19 mm diameter rods.

DSC and DMA experiments were conducted on specimens in both the as-received state and a T6 condition, i.e. solution heat-treated at 530 °C for 1.5 h, water-quenched to room temperature, pre-aged for 20 h at room temperature followed by ageing at 175 °C for 8 h.

For DSC studies a Du Pont 910 DSC unit with a Du Pont 2100 Thermal Analyser was employed using discs of the PMMC materials of 5 mm in diameter and 0.5–1.0 mm in thickness. The temperature range investigated was 25–535 °C, using a scan rate of 20 °C min^{-1}.

DMA studies were carried out with a Du Pont 983 Dynamic Mechanical Analyser and a Du Pont 2100 Thermal Analyser; version 6.0 software was used. Rectangular strips approximately $30 \times 12 \times 1.5$ mm were clamped between two parallel arms. Specimens could be subjected to constant stress, oscillatory stress or constant strain, depending on the experimental mode. Sample deformation was monitored by a linear variable displacement transducer (LVDT). In the present experiments a resonant frequency mode was utilized, in which the sample was displaced and set into oscillation. Normally, a system so displaced would oscillate at the system's resonant frequency with constantly decreasing amplitude due to the loss of energy (damping) within the sample. The amplitude signal from the LVDT was used to control the output signal of the electromechanical driver. The driver supplied additional energy to the driving arm forcing the

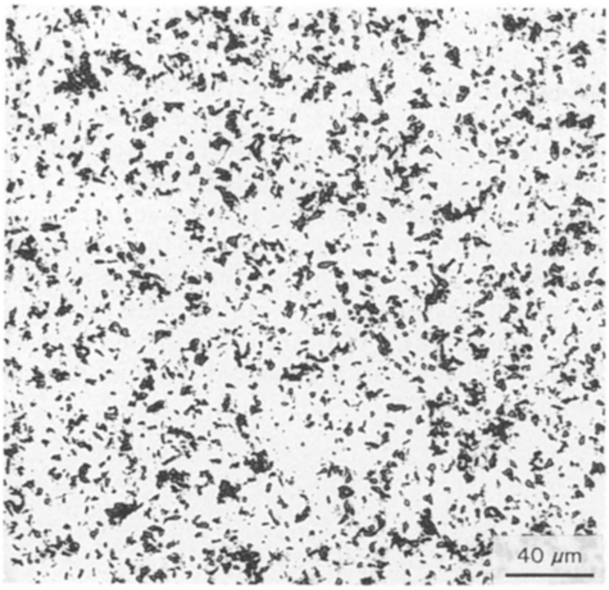

Figure 1 Optical micrograph of 6061 + 10 vol % SiC.

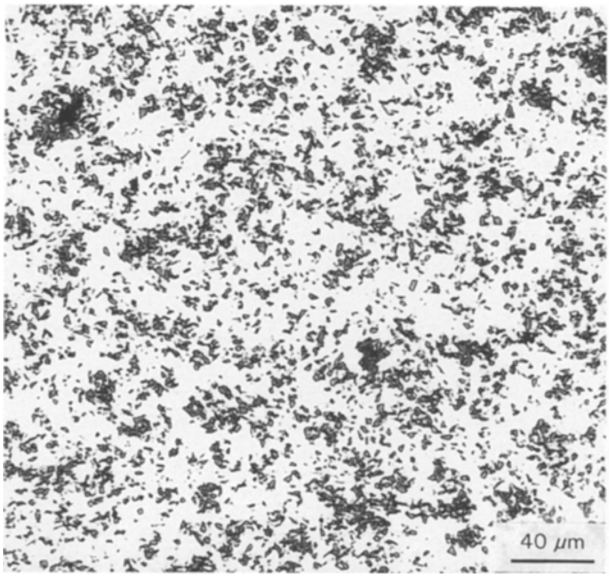

Figure 2 Optical micrograph of 6061 + 20 vol % SiC.

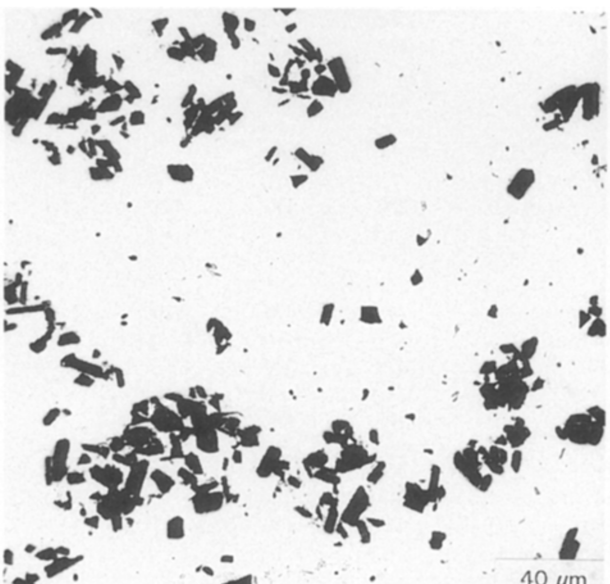

Figure 3 Optical micrograph of 6061 + 10 vol % Al_2O_3.

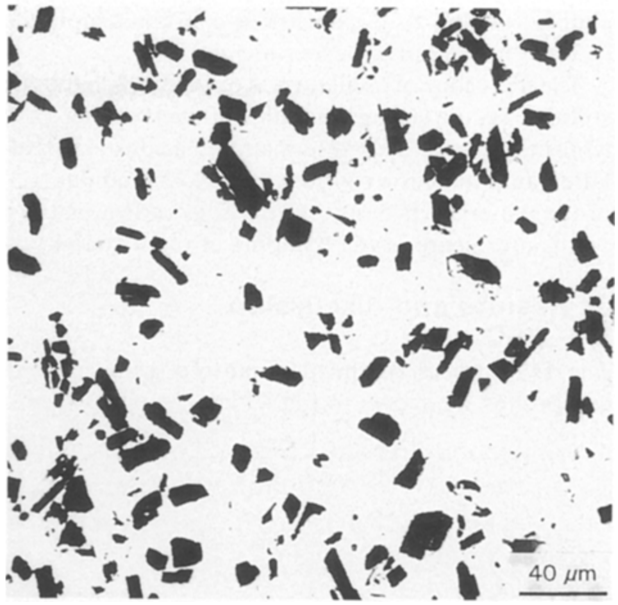

Figure 4 Optical micrograph of 6061 + 15 vol % Al_2O_3.

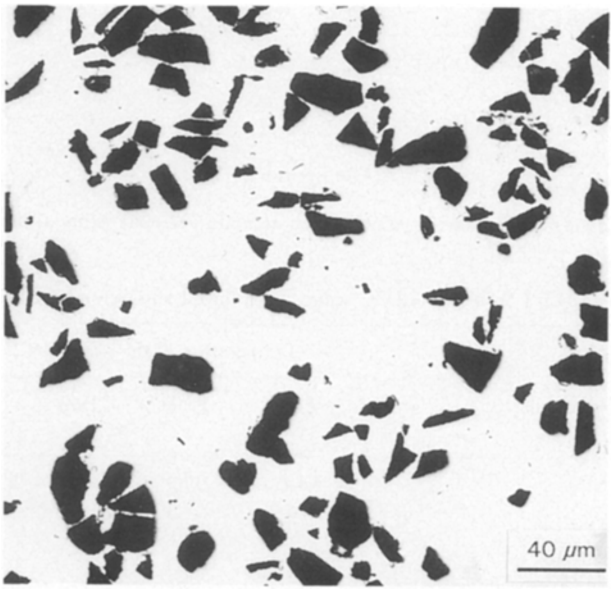

Figure 5 Optical micrograph of 6061 + 20 vol % Al_2O_3.

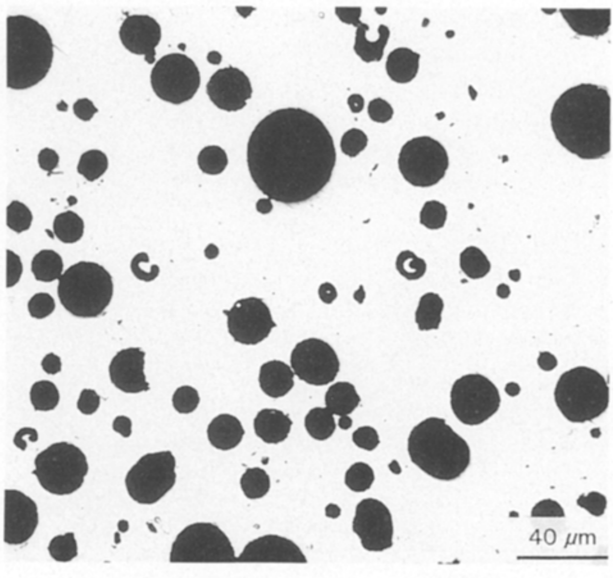

Figure 6 Optical micrograph of 6061 + 20 vol % Al_2O_3 (Micro-Sphere), Comral-85.

coupled system to oscillate at a constant amplitude (0.3 mm in the present experiments).

The frequency of oscillation is directly related to the stiffness, i.e. the storage modulus of the specimen (E'), whilst the energy needed to maintain a constant oscillation amplitude is a measure of the loss modulus (E'') of the material. The ratio of E''/E' is known as tan δ and is a measure of the damping of the material.

3. Results and discussion
3.1. DSC
The DSC traces of the unreinforced alloy and six composites are shown in Fig. 7–13. The peaks identified in these figures and the corresponding temperatures are presented in Table I. The peaks in these figures were determined with respect to the base lines (not shown in the figures). Some peaks were more prominent than the others, appearing over a broad range of temperatures and, in this case, peaks were identified at the average of the maxima and minima of temperatures in that range. It is noted that, in general, the peaks were more prominent in the case of specimens heat-treated to a T6 condition, with the exception of unreinforced 6061 and composite 6 where the peaks were also quite pronounced in the as-received condition.

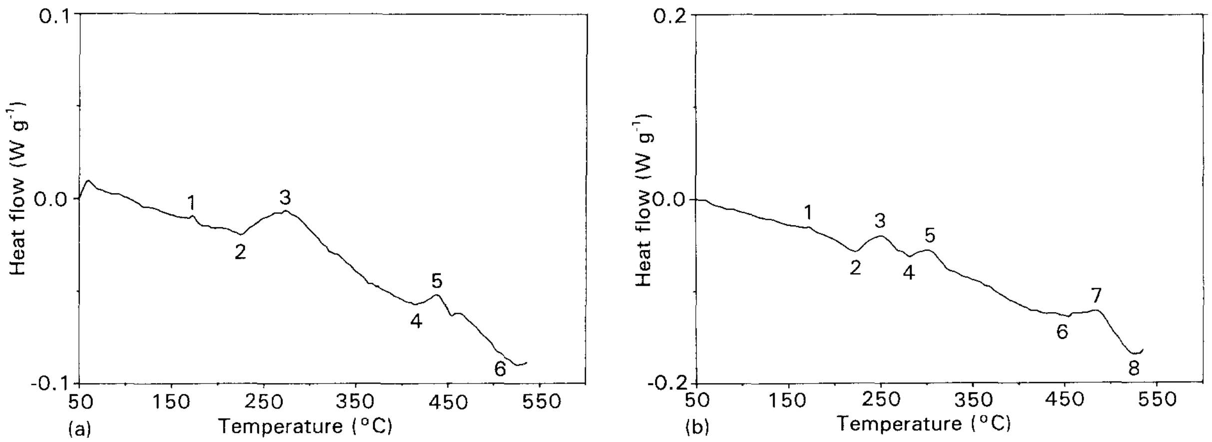

Figure 7 DSC thermograms of the unreinforced 6061 Al in (a) the as-received and (b) the T6 conditions.

TABLE I Analysis of DSC scans of reinforced and unreinforced 6061 Al-alloys

Materials	Fig.	Temperature of the peaks[c] (°C) Peak 1	Peak 2	Peak 3	Peak 4	Peak 5	Peak 6	Peak 7	Peak 8
6061	ASR[a]	170	225	270	405	445	525		
	7a	(+)[c]	(−)[c]	(+)	(−)	(+)	(−)		
	T6[b]	170	220	250	280	305	455	485	525
	7b	(+)	(−)	(+)	(−)	(+)	(−)	(+)	(−)
10 vol % SiC	ASR	170	220	270	320	450			
	8a	(+)	(−)	(+)	(+)	(−)			
	T6	170	220	275	290	350	530		
	8b	(+)	(−)	(+)	(+)	(+)	(−)		
20 vol % SiC	ASR	170	220	275	320	475	500	530	
	9a	(+)	(−)	(+)	(+)	(−)	(+)	(−)	
	T6	170	220	275	285	470	520		
	9b	(+)	(−)	(+)	(+)	(−)	(+)		
10 vol % Al_2O_3	ASR	170	220	275	535				
	10a	(+)	(−)	(+)	(−)				
	T6	170	225	245	260	280	450	485	520
	10b	(+)	(−)	(+)	(−)	(+)	(−)	(+)	(−)
15 vol % Al_2O_3	ASR	170	220	245	525				
	11a	(+)	(−)	(+)	(−)				
	T6	170	220	250	290	445	470	520	
	11b	(+)	(−)	(+)	(+)	(−)	(+)	(−)	
20 vol % Al_2O_3	ASR	170	220	275	420	470	520		
	12a	(+)	(−)	(+)	(−)	(+)	(−)		
	T6	170	220	250	300	455	490	530	
	12b	(+)	(−)	(+)	(+)	(−)	(+)	(−)	
Comral-85	ASR	170	200	260	375	500			
	13a	(+)	(−)	(+)	(−)	(+)			
	T6	170	220	245	295	455	490	535	
	13b	(+)	(−)	(+)	(+)	(−)	(+)	(−)	

[a]ASR, As-received.
[b]T6, T6 heat-treated condition.
[c](+), Exothermic; (−), endothermic.

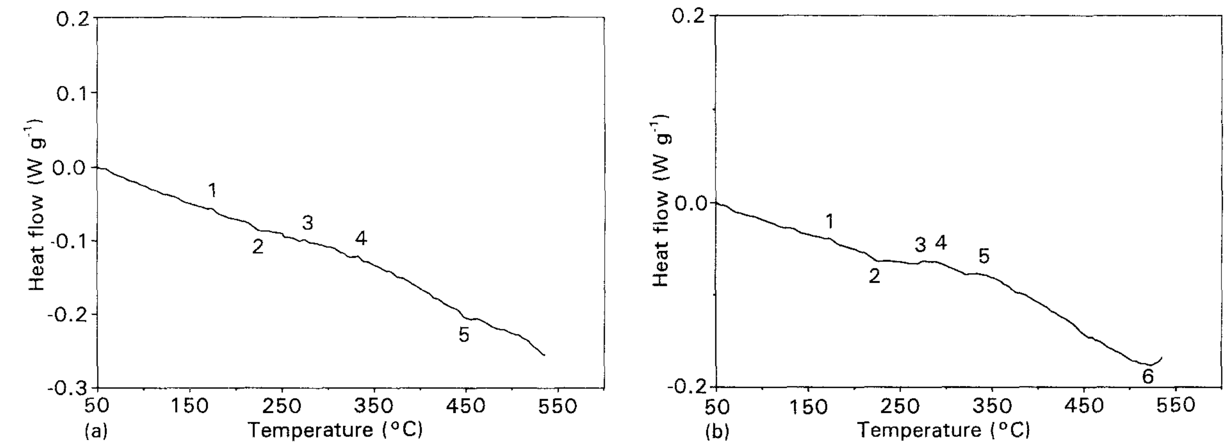

Figure 8 DSC thermograms of the 10 vol % SiC/6061 composite in (a) the as-received and (b) the T6 conditions.

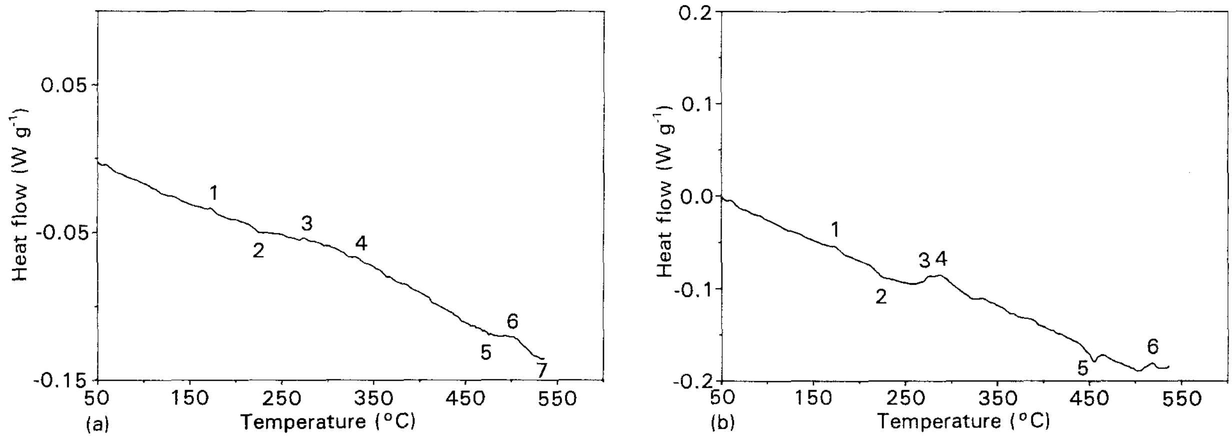

Figure 9 DSC thermograms of the 20 vol % SiC/6061 composite in (a) the as-received and (b) the T6 conditions.

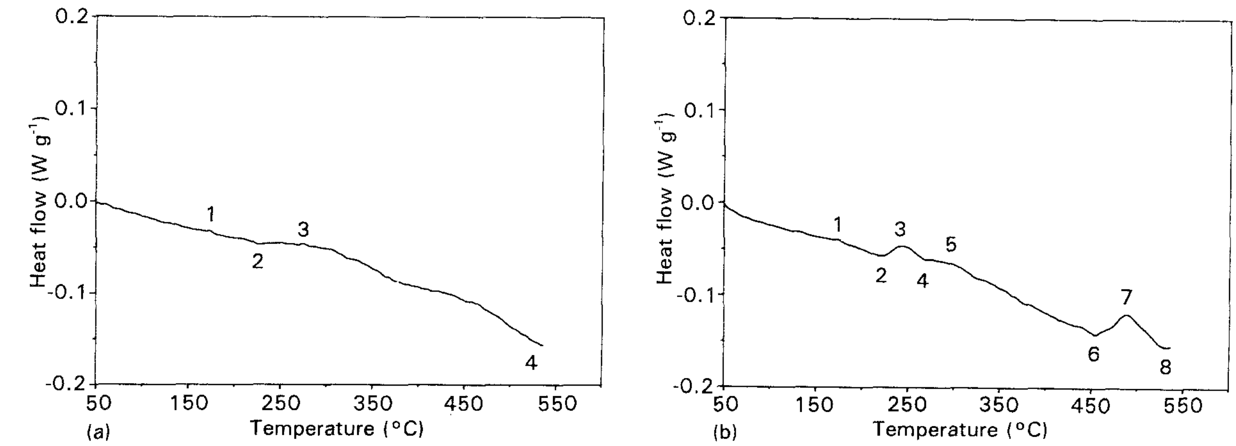

Figure 10 DSC thermograms of the 10 vol % Al_2O_3/6061 composite in (a) the as-received and (b) the T6 conditions.

As can be seen in Table I, all the materials showed a weak exothermic peak, e.g. peak 1 at 170 °C, and a weak endothermic peak, e.g. peak 2 at 220 °C, most likely due to the formation and dissolution of the GP zones (as observed by Badini and co-workers [6, 8]), respectively.

Exothermic peak 3 was seen in all materials and occurred in the temperature range of 245–275 °C. It is believed that this peak was due to the formation of metastable (β″) and stable (β′) precipitates [6]. It is interesting to note that in materials 1 and 2 this peak was closely followed by another exothermic peak (peak 4) in both the as-received and T6 specimens. In materials 3–7 this exothermic peak was seen to occur only in the T6 treated specimens. In materials 3 and 7 this peak is denoted as peak 5, but in materials 4–6 as peak 4. Peaks 3 and 4 for materials 1, 2 and 4–6, and peaks 3 and 5 for materials 3 and 7, are considered to

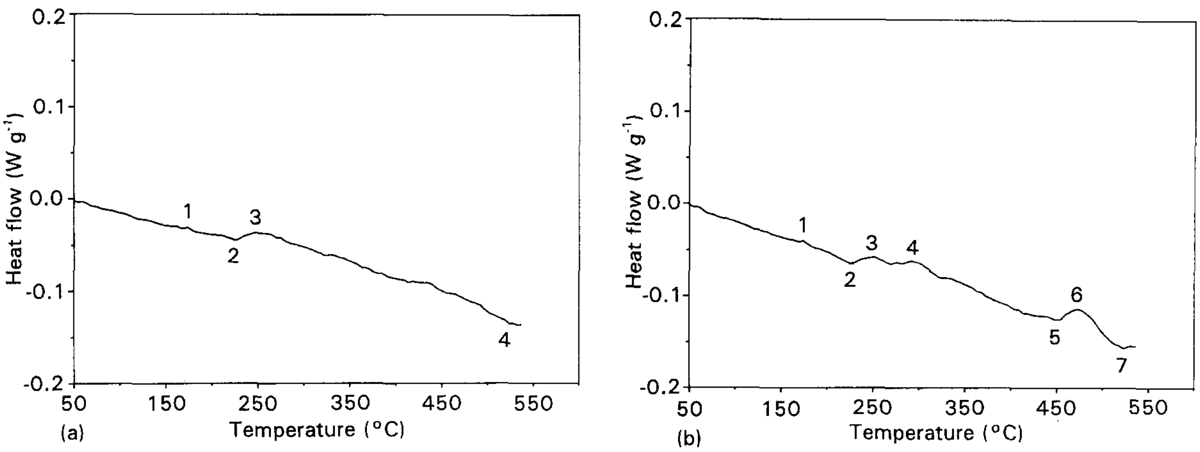

Figure 11 DSC thermograms of the 20 vol % Al_2O_3/6061 composite in (a) the as-received and (b) the T6 conditions.

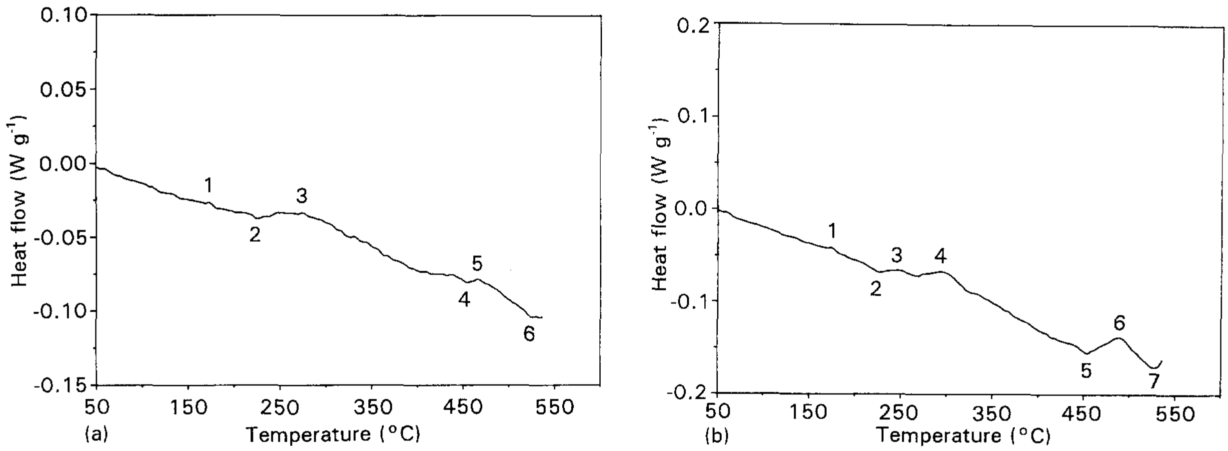

Figure 12 DSC thermograms of the 15 vol % Al_2O_3/6061 composite in (a) the as-received and (b) the T6 conditions.

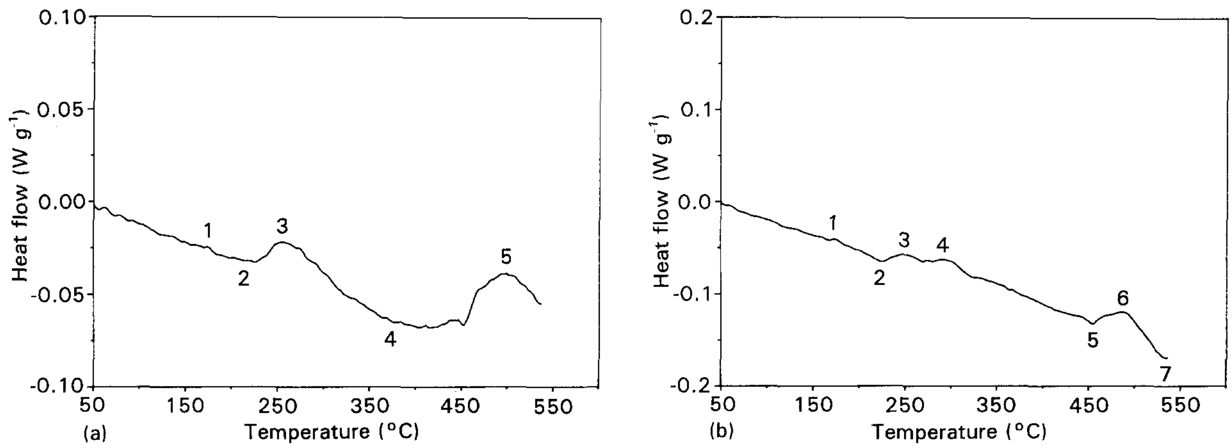

Figure 13 DSC thermograms of the 20 vol % Al_2O_3/6061 (Comral-85) in (a) the as-received and (b) the T6 conditions.

be due to the peak age-hardening phenomenon, as has been confirmed in a TEM study by Dutta and Bourell [9]. From Figs 7 to 13 it is observed that for all the PMMC materials examined (1–6), the β'' and β' transformations in the ageing sequence occurred at lower temperatures as compared to the 6061 matrix alloy (peaks 3 and 5: 250 and 305 °C), hence the precipitation reactions in composites appeared to occur much faster than in the unreinforced alloy.

A large and complex endothermic area appeared for all the materials (followed by the above two exotherms) which is believed to be due to the dissolution of precipitates [8], this occurs at a temperature of $\sim$450 °C. Immediately after this an exothermic peak appeared at a relatively high temperature, 480 °C for the T6 materials, possibly due to formation of equilibrium precipitates (incoherent β-phase), which was again followed by the endotherm, possibly associated with the dissolution of the equilibrium of β precipitates [7], this temperature was close to the solutionizing temperature (530 °C) for the matrix alloys. For 6061, 10 vol % Al_2O_3, 15 vol % Al_2O_3, 20 vol % Al_2O_3 and Comral-85, this exothermic peak appeared at almost the same temperature (485 °C), Figs 7–13, part b. A slight deviation was found for 20 vol % SiC where the peak appeared at 520 °C, and no such peak was found to exist in the case of 10 vol % SiC.

From the overall results, it can be seen that the formation of equilibrium precipitates was insensitive to the amount and type of reinforcement present in the matrix alloy, however, the peak age-hardening phenomenon, due to the formation of coherent precipitates, was very sensitive to the amount and type of reinforcement.

The faster ageing process may be explained [9] in terms of dislocations present in the matrix and those dislocations which are generated due to the thermal mismatch between the ceramic particles and the matrix alloy, induced as a result of quenching from the solutionizing temperature, 530 °C. For irregular-shaped particles (in the case of SiC and Al_2O_3 reinforced composites) the stress concentrated corners were favourable sites for dislocation generation as compared to Comral-85 which contains Al_2O_3 microspheres. Hence, the dislocation density in the matrices of 20 vol % SiC and Al_2O_3 composites was greater than that in Comral-85 and so they aged faster than the latter. Future TEM studies on the above materials will help to quantify this phenomenon.

3.2. DMA

It is evident from Figs 14 to 16 that E' of both the unreinforced and reinforced 6061 Al-alloys decreased with increasing temperature for materials as-received and in the T6 condition.

Figs 14–16, part a, indicate DMA results in the as-received condition for 10 and 20 vol % SiC, 10 and 20 vol % Al_2O_3, 15 vol% Al_2O_3 and Comral-85, respectively. In the above figures the E' data are compared with those of the as-received 6061 matrix alloy. Figs 14–16, part b, indicate results for the same materials in the T6 condition. In general, the storage modulus of the composites appeared to be dependent on the volume fraction of the reinforcement in the matrix alloy. Absolute values of E' at room temperature for all materials examined in the study were consistently lower ($\sim$18 GPa) than corresponding values reported in the literatures for such materials [10–12]. The reason for this difference is not known; however, as present interest is in the change of E' with temperature, this discrepancy will be ignored, and the

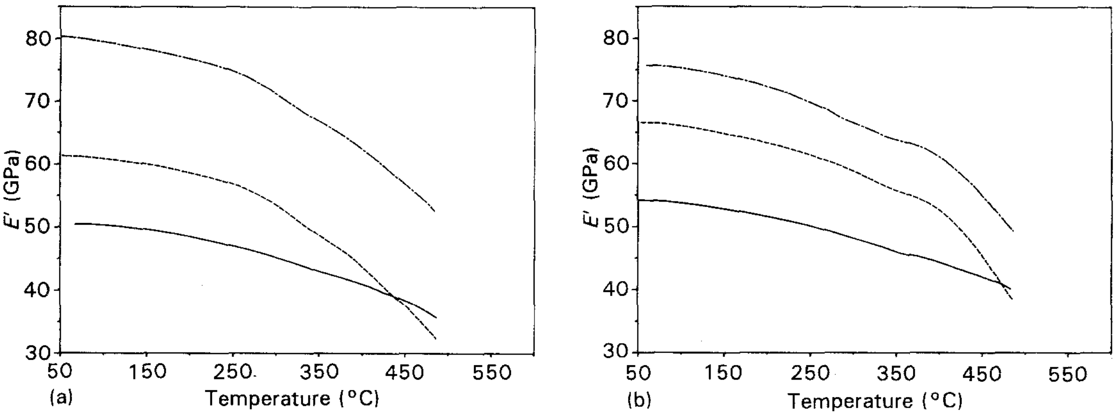

Figure 14 Temperature dependence of E' for 10 (---) and 20 vol % (-··-) SiC/6061 in comparison to 6061 (-) Al in (a) the as-received and (b) the T6 conditions.

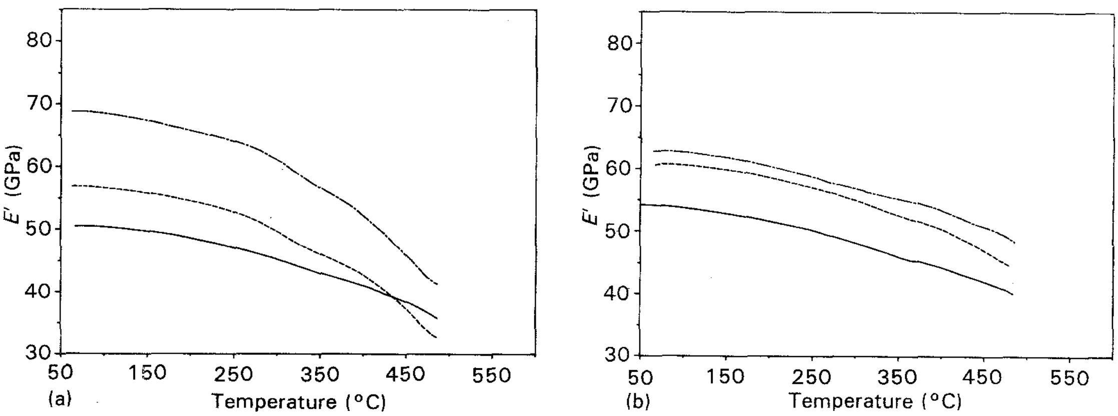

Figure 15 Temperature dependence of E' for 10 (---) and 20 vol % (-··-) Al_2O_3/6061 in comparison to 6061 (—) Al in (a) the as-received and (b) the T6 conditions.

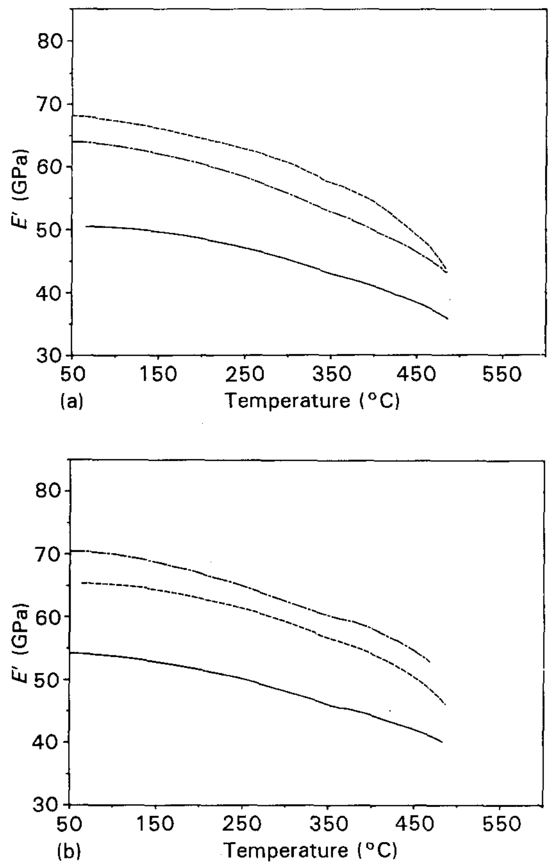

Figure 16 Temperature dependence of E' for 15 vol % Al_2O_3 (---) and Comral-85 (-·-) in comparison to 6061 (—) Al in (a) the as-received and (b) the T6 conditions.

change in E' as a function of temperature, as shown in Figs 14–16, will be considered.

In Table II, E' values are presented at various temperatures for the materials in both the as-received and the T6 condition for ranking purposes. From this table it can be seen that 20 vol % SiC composite (no. 2) retained the highest modulus at all temperatures in both conditions. The next in ranking in the as-received condition was generally the 20 vol % Al_2O_3 composite (no. 5), however, in the T6 condition, Comral-85 (no. 6) took a higher ranking, next to 20 vol % SiC. The other composites showed some changes in their ranking, but the 6061 unreinforced alloy had the lowest modulus in both conditions and at all temperatures, which illustrates the beneficial aspect of reinforcement in so far as high temperature is concerned.

Whilst the question of improved moduli in PMMCs is often addressed from the rule of mixtures, the effect of interfacial factors as well as the precipitation mechanisms in the matrix on E' may not be totally ruled out. However, this needs a more detailed examination of the microstructure and the interface, and this will be looked at in the future.

E'' and tan δ generally provide information regarding transformation changes [13] and damping in materials. E'' and tan δ plots for 20 vol % SiC both in the as-received and the T6 treated conditions, are shown in Fig. 17a and b respectively. The temperatures at which maxima (point of inversion) in tan δ are observed for materials 1–7 are listed in Table III. The

TABLE II Ranking of materials (E') at various temperatures from Figs 14–16, highest ranking at the top

Heat-treatment	Temperature (°C) 100	150	200	250	300	350	400
As-received	20 vol % SiC/6061	20 vol % SiC/6061	20 vol % SiC/6061	20 vol % SiC/6061	20 vol % SiC/6061	20 vol % SiC/6061	20 vol % SiC/6061
	20 vol % Al_2O_3/6061	20 vol % Al_2O_3/6061	20 vol % Al_2O_3/6061	20 vol % Al_2O_3/6061	20 vol % Al_2O_3/6061	20 vol % Al_2O_3/6061	15 vol % Al_2O_3/6061
	15 vol % Al_2O_3/6061	15 vol % Al_2O_3/6061	15 vol % Al_2O_3/6061	15 vol % Al_2O_3/6061	15 vol % Al_2O_3/6061	15 vol % Al_2O_3/6061	20 vol % Al_2O_3/6061
	Comral-85	Comral-85	Comral-85	Comral-85	Comral-85	Comral-85	Comral-85
	10 vol % SiC/6061	10 vol % SiC/6061	10 vol % SiC/6061	10 vol % SiC/6061	10 vol % SiC/6061	10 vol % SiC/6061	10 vol % SiC/6061
	10 vol % Al_2O_3/6061	10 vol % Al_2O_3/6061	10 vol % Al_2O_3/6061	10 vol % Al_2O_3/6061	10 vol % Al_2O_3/6061	10 vol % Al_2O_3/6061	10 vol % Al_2O_3/6061
	6061	6061	6061	6061	6061	6061	6061
T6 condition	20 vol % SiC/6061	20 vol % SiC/6061	20 vol % SiC/6061	20 vol % SiC/6061	20 vol % SiC/6061	20 vol % SiC/6061	20 vol % SiC/6061
	Comral-85	Comral-85	Comral-85	Comral-85	Comral-85	Comral-85	Comral-85
	10 vol % SiC/6061	10 vol % SiC/6061	10 vol % SiC/6061	10 vol % SiC/6061	15 vol % Al_2O_3/6061	15 vol % Al_2O_3/6061	15 vol % Al_2O_3/6061
	15 vol % Al_2O_3/6061	15 vol % Al_2O_3/6061	15 vol % Al_2O_3/6061	15 vol % Al_2O_3/6061	10 vol % SiC/6061	10 vol % SiC/6061	20 vol % Al_2O_3/6061
	20 vol % Al_2O_3/6061	20 vol % Al_2O_3/6061	20 vol % Al_2O_3/6061	20 vol % Al_2O_3/6061	20 vol % Al_2O_3/6061	20 vol % Al_2O_3/6061	10 vol % SiC/6061
	10 vol % Al_2O_3/6061	10 vol % Al_2O_3/6061	10 vol % Al_2O_3/6061	10 vol % Al_2O_3/6061	10 vol % Al_2O_3/6061	10 vol % Al_2O_3/6061	10 vol % Al_2O_3/6061
	6061	6061	6061	6061	6061	6061	6061

TABLE III Phase changes from DSC plots at the temperatures where maximum of tan δ observed in DMA experiment

Materials	As-received		T6-treated	
	Temp. at max. of tan δ from DMA (°C)	Phase changes at max. of tan δ from DSC	Temp. at max. of tan δ from DMA (°C)	Phase changes at max. of tan δ from DSC
6061	335	Dissolution of β″ and β′	370	Dissolution of β″ and β′
10 vol % SiC/6061	325	Formation of β′	330	Formation of β′
20 vol % SiC/6061	320	Formation of β′	285	Formation of β′
10 vol % Al_2O_3/6061	325	Formation of β′	360	Dissolution of β′
15 vol % Al_2O_3/6061	340	Dissolution of β′	325	Dissolution of β′
20 vol % Al_2O_3/6061	335	Dissolution of β′	335 (Not prominent)	Dissolution of β′
20 vol % Al_2O_3(MS)/ 6061	330	Dissolution of β′	330 (Not prominent)	Dissolution of β′

β′, Stable precipitates; β″ metastable precipitates; tan δ = E''/E'.

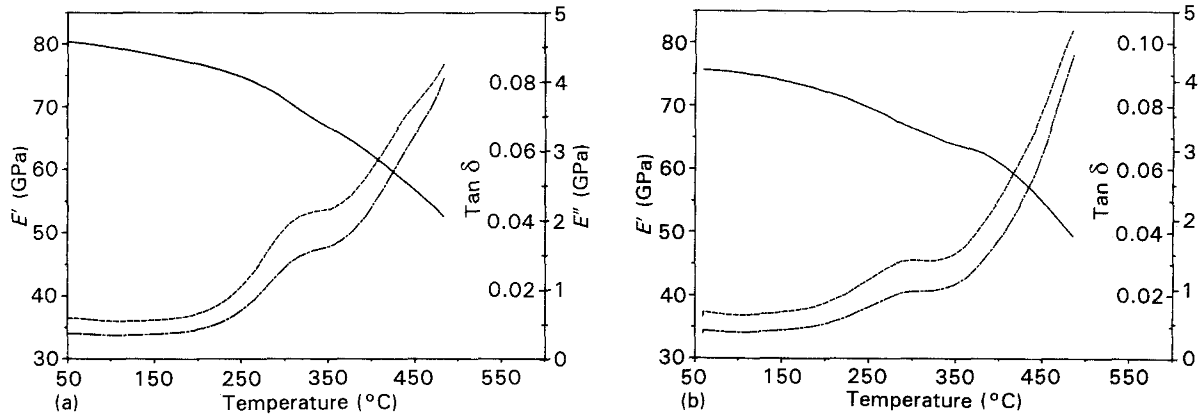

Figure 17 E' (——), E'', (– – –) and tan δ (---) plots as a function of temperature for 20 vol % SiC/6061 in (a) the as-received and (b) the T6 conditions.

maxima are considered to relate to a transformation process in the material and are obtained from the corresponding DSC plots (also noted in Table III). In case of as-received 6061, 15 vol % Al_2O_3, 20 vol % Al_2O_3 and Comral-85, the maxima of tan δ appeared at 330–340 °C and were found to be due to the dissolution of β′ precipitates from the corresponding DSC plots. For 10 vol % SiC, 20 vol % SiC and 10 vol % Al_2O_3 in the as-received condition, the maxima appeared at slightly lower temperatures, 320–325°C, and were found to correlate with the formation of β′ precipitates. However, materials in the T6 condition showed a different behaviour. The maxima of tan δ for 6061, 10 vol % Al_2O_3, 15 vol % Al_2O_3, 20 vol % Al_2O_3 and Comral-85 occurred over a wider range of temperatures, from 330 to 370 °C, and were apparently due to the dissolution of β′ precipitates. Also, for 10 and 20 vol % SiC the maxima occurred from 285 to 330 °C and were due to the formation of β′ precipitates. The only exceptions were found for 20 vol % Al_2O_3 and Comral-85 where the peaks of tan δ were not prominent in the T6 condition. However, the confirmation of the phase changes at the maxima of tan δ needs further study, including TEM work, which is in progress.

4. Conclusions

From the DSC and DMA studies presented the following conclusions may be drawn:

1. The formation of equilibrium β precipitates is insensitive to the amount and type of reinforcement (SiC, Al_2O_3) present in the matrix alloy (6061).
2. Peak age-hardening, which is due to the formation of coherent β′ precipitates, is sensitive to the amount and type of reinforcement.
3. Twenty vol % SiC/6061 retains the highest storage modulus E at all temperatures in both T6 and as-received conditions, whereas 6061 has the lowest E'.
4. From a combined study of DSC and DMA it is possible to identify the phase(s) /change(s) responsible for the maximum damping properties of the materials.

Acknowledgements

The authors wish to thank Drs Malcolm Couper and Kenong Xia of Comalco Research Centre, Thomastown, Victoria, for providing the materials used in these experiments. The work was presented at the 3rd Australian Forum on Metal Matrix Composites held at the University of New South Wales, Australia, 7 December, 1992.

References

1. A. MORTENSEN in Proceedings of "Fabrication of particulate reinforced metal composites", Montreal, Canada, Sept. 1990, Ed. J. Masounave and F. G. Hamel, published by ASM International, Materials Park, Ohio, USA, p. 217, 1990.
2. D. L. McDANELS, *Metall. Trans.* **16A** (1985) 1105.
3. J.-P. COTTU, J.-J. CONDERC, B. VIGUIER and L. BERNARD, *J. Mater. Sci.* **27** (1992) 3068.
4. C. M. FRIEND and S. D. LUXTON, *J. Mater. Sci.* **23** (1988) 3173.
5. J. L. PETTY-GALIS and R. D. GOOLSBY, *J. Mater. Sci.* **24** (1989) 1439.
6. P. APPENDINO, C. BADINI, F. MARINO and A. TOMASI, *Mater. Sci. Eng.* **A135** (1991) 275.
7. I. DUTTA, S. M. ALLEN and J. L. HAFLEY, *Metall. Trans. A* **22A** (1991) 2553.
8. C. BADINI, F. MARINO and A. TOMASI, *J. Mater. Sci.* **26** (1991) 6279.
9. I. DUTTA and D. L. BOURELL, *Mater. Sci. Engng.* **A112** (1989) 67.
10. J. A. DICARLO and J. E. MAISEL, Composite Materials: Testing and Design (Fifth Conference), ASTM STP 674, Ed. S. W. Tsai, ASTM, p. 201, 1979.
11. A. WOLFENDEN and J. M. WOLLA, *J. Mater. Sci.* **24** (1989) 3205.
12. J. M. WOLLA and A. WOLFENDEN, ASTM STP 1045, Ed. A. Wolfenden, ASTM, Philadelphia, p. 110, 1990.
13. C. D. ARMENIADES and E. BAER, in "Introduction to polymer science and technology", an SPE textbook, edited by H. S. Kaufman (A. Wiley-Interscience, New York, 1977) Ch. 6, p. 239.
14. M. P. SEPE, *Adv. Mater. Process.* **4** (1992) 32.
15. T. DAS, S. BANDYOPADHYAY and S. BLAIRS, *J. Mater. Engng. and Perf.* **1** (6) 1992) 839.

Received 18 March 1993
and accepted 8 March 1994